Structural characterization of an all-aminosugar-containing capsular polysaccharide from *Colwellia psychrerythraea* 34H

Angela Casillo, Jonas Ståhle, Ermenegilda Parrilli, Filomena Sannino, Daniel E. Mitchell, Giuseppina Pieretti, Matthew I. Gibson, Gennaro Marino, Rosa Lanzetta, Michelangelo Parrilli, Göran Widmalm, Maria L. Tutino, Maria M. Corsaro

Angela Casillo, Ermenegilda Parrilli, Filomena Sannino, Giuseppina Pieretti, Gennaro Marino, Rosa Lanzetta, Maria L. Tutino, Maria M. Corsaro (Corresponding author)
Department of Chemical Sciences, University of Naples "Federico II", Complesso Universitario Monte S. Angelo, Via Cintia 4, 80126 Naples, Italy
corsaro@unina.it

Jonas Ståhle, Göran Widmalm
Department of Organic Chemistry, Arrhenius Laboratory, Stockholm University, Stockholm, S-106 91, Sweden

Daniel E. Mitchell, Matthew I. Gibson
Department of Chemistry and Warwick Medical School, University of Warwick, Coventry, CV4 7AL, UK

Michelangelo Parrilli
Department of Biology, University of Naples "Federico II", Complesso Universitario Monte S. Angelo, Via Cintia 4, 80126 Naples, Italy.

Abstract

Colwellia psychrerythraea strain 34H, a Gram-negative bacterium isolated from Arctic marine sediments, is considered a model to study the adaptation to cold environments. Recently, we demonstrated that *C. psychrerythraea* 34H produces two different extracellular polysaccharides, a capsular polysaccharide and a medium released polysaccharide, which confer cryoprotection to the bacterium. In this study, we report the structure of an additional capsular polysaccharide produced by *Colwellia* grown at a different temperature. The structure was determined using chemical methods, and one- and two-dimensional NMR spectroscopy. The results showed a trisaccharide repeating unit made up of only amino-sugar residues: *N*-acetyl-galactosamine, 2,4-diacetamido-2,4,6-trideoxy-glucose~~pyranose~~ (bacillosamine), and 2-acetamido-2-deoxyglucuronic acid with the following structure: →4)-β-D-Glc*p*NAcA-(1→3)-β-D-Qui*p*NAc4NAc-(1→3)-β-D-Gal*p*NAc-(1→. The 3D model, generated in accordance with ^{1}H,^{1}H-NOE NMR correlations and consisting of ten repeating units, shows a helical structure. In contrast with the other ~~exopolysaccharides~~ extracellular polysaccharides produced from *Colwellia* at 4 °C, this molecule displays only a low ice recrystallization inhibition activity.

Keywords

Cold adaptation, Extracellular polysaccharides, NMR, Psychrophile, Anti-freeze activity

Introduction

Life on Earth has evolved to colonize low-temperatures environments, characterized by temperatures that are close to or below the freezing point of water (Bakermans et al. 2004). Permanently cold environments cover about one-fifth of the Earth's surface and include Arctic and Antarctic regions, polar and alpine habitats, the deep oceans, permafrost, and lake ice. Subzero temperatures pose a significant challenge to the survival of several organisms, including representatives of the *Bacteria*, *Archea*, and *Eucarya* (Cavicchioli et al. 2000). These extreme conditions impose severe physicochemical constrains on cellular function, by negatively influencing cell integrity, membrane fluidity, and macromolecular interactions (De Mayeer et al. 2014). Therefore, the ability of an organism to survive and grow in cold conditions depends on a pool of adaptive strategies, involving all the components of the microbial cell, from membranes and transport system to intracellular solutes. In recent years, among the well-known membrane responses to cold, an increasing attention has been given to the extracellular polysaccharides ~~exopolysaccharides (EPSs)~~ produced by bacteria in sea ice (Mancuso et al. 2005; Ewert et al. 2013). Chemically, these polymers are high-molecular weight ~~mass~~ polysaccharides, of which some are neutral, although polyanionic species are the most abundant, due to the high presence of uronic acids (commonly D-glucuronic acid, but D-galacturonic and D-mannuronic acids are also found) and/or anionic substituents (Poli et al. 2010). Bacterial extracellular polysaccharides ~~EPSs~~ usually occur in two forms: i) either strictly associated to the cell surface (capsular polysaccharides, CPS) (Kumar et al. 2007); ii) and/or ~~as slime polysaccharides that either remain attached (loosely bound) to the cell surface or are found~~ secreted in the extracellular medium as an amorphous matrix (exopolysaccharides, EPS) (Sutherland 1982; Decho et al. 1990). The ability of a microorganism to surround itself with a highly hydrated shell helps to buffer the cell against the osmotic stress of high salt concentrations, and may provide it with protection against desiccation and predation by protozoans (Kumar et al. 2007). Therefore, ~~EPSs~~ extracellular polysaccharides are essential in the aggregate formation, in the mechanism of adhesion to surfaces, in the uptake of nutrients (Poli et al. 2010), and are involved in host-pathogen interplay (Kadioglu et al. 2008; de Pinto et al. 2003). Moreover, ~~EPSs~~ extracellular polysaccharides are common components of biofilm and their production is an important feature of the mature biofilm (Fux et al. 2003).

Liu et al. (2013) suggested that extracellular polysaccharides, produced by psychrophilic microorganisms, do play a role in the mechanism of cryoprotection. This role has been definitively established in *Colwellia psychrerythraea* 34H (Casillo et al. 2017 and references therein), a psychrophilic γ-proteobacterium isolated from Arctic marine sediments (Methè et al. 2005; Deming et al. 1988). *C. psychrerythraea* 34H is considered the type species of the genus *Colwellia* (Deming 1988), and its genome was the first obtained from an obligate psychrophile. As a result, the 34H genome has proven to be very useful for understanding the features that allow for life at freezing temperatures (Bowman et al. 2014). *C. psychrerythraea* grows in a temperature range of approximately -1 °C to 10 °C, with cardinal growth optimum temperatures of 8 °C (Huston et al. 2004). Recently, we determined the structure of both capsular (Carillo et al. 2015) and medium released polysaccharides (Casillo et al. 2017) produced by *C. psychrerythraea* when grown at 4 °C. Here we describe the primary structure and the three-dimensional model of a new CPS polysaccharide, strictly associated to the cell surface, produced by the bacterium when grown at 8 °C. In contrast with the other extracellular polysaccharides produced from *Colwellia* at 4 °C, this molecule is not decorated with any amino acid residue and displays only a low ice recrystallization inhibition activity.

Materials and methods

Cell growth

C. psychrerythraea 34H was grown aerobically at 8 °C in Marine Broth medium (DIFCO™ 2216). When the liquid culture reached late exponential phase (OD600 = 2), cells were harvested by centrifugation for 20 min at 5000 rpm and 4 °C.

CPS isolation and purification

Dried cells (0.6 g) were extracted first with phenol/chloroform/light petroleum (PCP) method to recover lipooligosaccharide (LOS), and then by hot phenol/water method as reported previously (Carillo et al. 2015; Carillo et al. 2013). A 100 mg amount of water extract was dialyzed and then digested with proteases, DNAses and RNAses to remove contaminating proteins and nucleic acids. The water extract was hydrolysed with 5% aqueous CH_3COOH (5 mL, 100 °C, 5 h). The resulting suspension was then centrifuged (10,000×*g*, 4 °C, 30 min). The pellet was washed twice with water and the supernatant layers were combined and lyophilized (56 mg). The supernatant portion was then fractionated on a Biogel P-10 column (Biorad, 1.5 × 130 cm, flow rate 17 $mL \cdot h^{-1}$, fraction volume 2.5 mL), eluted with water buffered with 0.05 M pyridine and 0.05 M acetic acid (pH 5.0), obtaining two fractions. The first, eluted with the void volume, contained a polysaccharide material (36 mg), while the second contained oligosaccharides (15 mg). The polysaccharide material was further purified on a Sephacryl S-400HR (GE Healthcare Life Sciences, 1 × 110 cm, flow rate 15.6 $mL \cdot h^{-1}$, fraction volume 2.5 mL) eluted with 0.05 M ammonium hydrogen carbonate, providing a major fraction containing a fairly pure polysaccharide (CPS, 16 mg). The sugar-containing portion was further purified on a Q-Sepharose fast flow ion exchange chromatography (GE Healthcare Life Sciences, 1 × 35 cm, flow rate 23 $mL \cdot h^{-1}$, fraction volume 2 mL) eluted with 0.1 to 1 M NaCl. After dialysis against water, a pure fraction was obtained that contained the CPS (1 mg).

DOC-PAGE analysis

Polyacrylamide gel electrophoresis (PAGE) was performed using the system of Laemmli (Laemmli 1970) with sodium deoxycholate (DOC) as detergent. The separating gel contained final concentrations of 14% acrylamide, 0.1% DOC and 375 mM Tris/HCl (pH 8.8); the stacking gel contained 4% acrylamide, 0.1% DOC and 125 mM Tris/HCl (pH 6.8). EPS samples were prepared at a concentration of 0.05% in the sample buffer (2% DOC and 60 mM Tris/HCl [pH 6.8], 25% glycerol, 14.4 mM 2-mercaptoethanol, and 0.1% bromophenol blue). All concentrations are expressed as mass/vol percentage. The electrode buffer was composed of SDS (1 $g \cdot L^{-1}$), glycine (14.4 $g \cdot L^{-1}$) and Tris (3.0 $g \cdot L^{-1}$). Electrophoresis was performed at a constant amperage of 30 mA. Gels were fixed in an aqueous solution of 40% ethanol and 5% acetic acid. EPS bands were visualized by Alcian blue staining.

Sugar analysis

Monosaccharides were analysed as acetylated methyl glycosides, as reported previously (Pieretti et al. 2009). The absolute configuration of the sugars was determined by gas-chromatography analysis of their acetylated *(S)*-2-octyl glycosides (Leontein et al. 1978). All the samples were analyzed on an Agilent Technologies gas chromatograph 6850A equipped with a mass selective detector 5973N and a Zebron ZB-5 capillary column (Phenomenex, 30 m x 0.25 mm i.d., flow rate 1 $mL \cdot h^{-1}$, He as carrier gas). Acetylated methyl glycosides were analyzed accordingly with the following temperature program: 150 °C for 3 min, 150 °C→240 °C at 3 $°C \cdot min^{-1}$. Analysis of acetylated octyl glycosides was performed at 150 °C for 5 min, then 150 °C→240 °C at 6 $°C \cdot min^{-1}$, and 240 °C for 5 min.

NMR spectroscopy

Diffusion-edited proton NMR spectrum was recorded at 310 K by using a Bruker Avance II 500 MHz equipped with a 5 mm TCI Z-Gradient CryoProbe. ^{1}H and ^{13}C NMR spectra were recorded using Bruker Avance III 600 MHz and Bruker Avance III 700 MHz spectrometers equipped with a 5 mm TCI Z-Gradient CryoProbes. All two-dimensional homo- and heteronuclear experiments (double quantum-filtered correlation spectroscopy, DQF-COSY; total correlation spectroscopy TOCSY; nuclear Overhauser enhancement spectroscopy, NOESY; multiplicity-edited heteronuclear single quantum coherence, $^{1}H,^{13}C$-HSQC; heteronuclear multiple bond correlation, ^{1}H-^{13}C HMBC; band-selective constant time-HMBC, $^{1}H,^{13}C$-BSCT-HMBC; and 2D F_2-coupled HSQC) were performed at 278 K, 303 K or 310 K using standard pulse sequences available in the Bruker ~~software~~library. $^{1}H,^{1}H$-NOESY experiments were performed with mixing times from 30 to 300 ms, by using sodium 3-trimethylsilyl-(2,2,3,3-$^{2}H_4$)-propanoate (TSP, δ_H 0.00) as external reference. ^{13}C

NMR chemical shifts were referenced to external 1,4-dioxane in D_2O (δ_C 67.40). The temperature was calibrated with a neat deuterated methanol sample prior to experiments (Findeisen et al. 2007).

Molecular modeling

A 3D model of the CPS was built using the CarbBuilder v2.1.7 program (Kuttel et al. 2016) using default dihedral angles with ten repeating units as input. Atomic collisions due to steric crowding are handled automatically by first adjusting the ψ dihedral angle (C1'-O*n*-C*n*-H*n*, where *n* denotes the substitution position) by ± 10° and if the structure still contains clashes the next default dihedral value is used.

Ice recrystallization inhibition assay

Ice recrystallization inhibition (IRI) was measured using a modified splat assay (Congdon et al. 2013). A 10 μL sample of polymer dissolved in PBS buffer (pH 7.4) was dropped 1.40 m onto a chilled glass coverslip positioned on a piece of polished aluminum placed on dry ice. Upon hitting the chilled glass coverslip, a wafer with diameter of approximately 10 mm and thickness 10 μm was formed instantaneously. The glass coverslip was transferred onto the Linkam cryostage and held at −8 °C under N_2 for 30 min. Photographs were obtained using an Olympus CX 41 microscope with a UIS-2 20x/0.45/∞/0-2/FN22 lens and crossed polarizers (Olympus Ltd, Southend-on-Sea, UK), equipped with a Canon DSLR 500D digital camera. Images were taken of the initial wafer (to ensure that a polycrystalline sample had been obtained) and after 30 min. Image processing was conducted using Image J, which is freely available (http://imagej.net/). In brief, ten of the largest ice crystals were measured and the single largest length in any axis recorded. This was repeated for at least three wafers and the average (mean) value was calculated to find the largest grain dimension along any axis. The average of this value from three individual wafers was calculated to give the mean largest grain size (MLGS). This average value was then compared to that of a PBS buffer negative control providing a way of quantifying the amount of IRI activity.

Results and Discussion

Cell growth, CPS extraction and purification

The cells of *C. psychrerythraea* 34H grown at 8 °C were extracted by the PCP method (Galanos et al. 1969) in order to remove most of the LPS molecules, which interfere with the purification of the capsular polysaccharides. The PCP extract was analyzed by 14% DOC-PAGE and visualized by silver staining. The gel confirmed the presence of the rough lipopolysaccharide (LPS) already characterized for the bacterial cells grown at 4 °C (Carrillo et al. 2013) (data not shown). Thereafter, the remaining pellet was extracted by the phenol/water method (Westphal et al. 1965) and the water extract was dialyzed against water, and depleted of contaminants, such as proteins and nucleic acids, by using DNAse, RNAse and protease enzymatic digestion. The purified sample was analyzed by 14% DOC-PAGE and the gel visualized by Alcian blue staining. The staining revealed the presence of bands at low molecular masses attributable to the LPS molecules, and bands at high molecular masses attributable to the CPS (Fig. 1, lane a). The CPS from *Colwellia* grown at 8 °C is compared to that produced at 4 °C (Fig. 1, lane b). To overcome the troubles due to the aggregation of LPS and CPS molecules and to purify the polysaccharide component from these aggregates, the same procedure already used for the CPS isolated at 4 °C was applied (Carillo et al. 2015). After hydrolysis with 5% acetic acid and centrifugation, the supernatant mixture was purified by dialysis, gel permeation chromatography and ion exchange chromatography.

Structural characterization of CPS

The monosaccharide composition of the purified CPS, obtained by the GC-MS analysis of the acetylated methyl glycoside (MGA) derivatives showed the presence of 2-amino-2-deoxy-galactose (GalN) and 2-amino-2-deoxy-glucuronic acid (GlcNA). NMR analysis revealed the presence of an additional monosaccharide (see below). A D-configuration was identified for these two monosaccharides by the GC-MS analysis of the corresponding acetylated *(S)*-2-octyl glycosides. ~~(Leontein et al. 1978).~~ For the preparation of the GlcNA octyl glycoside standard, ~~we used the~~ *E. coli* monophosphoryl

lipid A was oxidized at position O-6 of the non-reducing glucosamine ~~*E. coli* monophosphoryl lipid A derivative was used~~ (D'Alonzo et al. 2016). After octanolysis followed by acetylation, we obtained the acetylated GlcNA octyl glycoside used as standard.

The polysaccharide was subsequently analyzed by one- and two-dimensional NMR spectroscopy techniques suitable for resonance assignments of carbohydrates (Widmalm 2007). The ^{1}H NMR spectrum of the CPS, recorded at 310 K, is shown in Figure 2. Three anomeric proton signals (**A-C**), attributable to CPS monosaccharide units, were present in the region between δ 4.6 and δ 4.4 (Table 1). In addition, four signals of acetyl groups occurred between 1.9 and 2.1 ppm, and a methyl signal, identified at 1.21 ppm, suggested the presence of a 6-deoxy sugar.

The chemical shifts of the ^{1}H and ^{13}C NMR resonances (Table 1) of the sugar residues in the repeating unit of the polysaccharide were assigned by 2D NMR spectroscopy experiments, complemented with chemical shift predictions made by the CASPER program (Jansson et al. 1989; Jansson et al. 1991).

Residue **A** with H-1/C-1 signals at δ 4.55/102.5 was identified as a *galacto*-configured residue based on the presence of cross-peaks from H-1 up to H-4 in the TOCSY spectrum; in the NOESY spectrum, starting from H-4, the resonances from H-5 and H-6 were assigned. Residue **A** was consequently assigned to a 3-substituted β-D-galactosamine residue as suggested by the large $^{3}J_{H1,H2}$ value (8.4 Hz) and a ^{1}H,^{13}C-HSQC correlation (Fig. 3) from its H-2 proton at 3.93 ppm to a nitrogen-bearing carbon at 51.8 ppm. The downfield chemical shift displacement of the C-3 resonance to 79.7 ppm identified its substitution position (Bock et al. 1983, Jansson et al. 1989). The H-2 proton was also shifted downfield indicating the presence of an acyl substituent on the amino group, identified as an *N*-acetyl group.

Residue **B** with H-1/C-1 signals at 4.47/103.1 ppm was assigned to a 2,4-diacetamido-2,4,6-trideoxy-β-D-glucopyranose (QuiNAc4NAc) residue, as suggested by the large $^{3}J_{H1,H2}$ value (8.0 Hz) and the occurrence in the HSQC spectrum of correlations of H-2 and H-4 signals at δ 3.78 and 3.56 with nitrogen-bearing carbons at δ 56.3 and 56.5, respectively, as well as a methyl group at δ_{H6}/δ_{C6} 1.21/17.9 (Fig. 3b). The cross-peaks from H-1 to H-6 in the TOCSY spectrum provided evidence for the *gluco*-configuration for this ring system. The downfield chemical shift displacement of C-3 value at 78.9 ppm identified its substitution position (Corsaro et al. 1999; ~~Pieretti et al. 2008~~). Moreover, the H-2 and H-4 signals were also shifted downfield indicating the presence of acyl substituents on the amino groups, which were found to be *N*-acetyl groups (Fig. 3c).

Residue **C**, with H-1/C-1 signals at δ 4.43/103.3, was identified as a 4-substituted GlcNAcA residue. The *gluco*-configured stereochemistry was suggested by the occurrence of strong scalar correlations in both COSY and TOCSY experiments; the β-configuration was identified from the large $^{3}J_{H1,H2}$ value (7.3 Hz), and the downfield chemical shift displacement of the C-4 resonance to 77.6 ppm identified its substituted position (Bock et al. 1983). The ^{1}H,^{13}C-HSQC spectrum (Fig. 3) revealed that the H-2 signal at 3.58 ppm correlated with a nitrogen-bearing carbon at 56.0 ppm, which carried an *N*-acetyl group as proven by the H-2 downfield chemical shift. Finally, long-range scalar correlations between both signals of H-5 and H-4 with a signal at 174.3 ppm in the ^{1}H,^{13}C-HMBC spectrum confirmed the C-6 carboxyl group assignment for this residue.

The D absolute configuration of the β-QuiNAc4NAc was established on the basis of the glycosylation effect of the ^{13}C NMR chemical shift values (Lipkind et al. 1988; Söderman et al. 1998). Specifically, ^{13}C chemical shift glycosylation methodology agrees well for the **B**→**A** structural element where both sugar residues have the D absolute configuration, e.g., $\Delta\delta_C$ is negative for C2, large and positive for C3, close to zero for C4 of →3)-β-D-Gal*p*NAc-(1→ (Table 1). The absolute configuration of residue **B** is not readily determined from the glycosylation shift of the anomeric carbon of residue **C**. However, that residue **C** has the D absolute configuration is supported by $\Delta\delta_C$ being negative for C3, large and positive for C4, whereas $\Delta\delta_{C5}$ does not differentiate the relative configuration between sugar residues. In addition, this is consistent with the slightly smaller glycosylation shift for the D absolute configuration of the anomeric carbon in residue **A**. Furthermore, in a structurally modified polysaccharide from *Bacillus licheniformis* ATCC 9945 a linear polysaccharide was prepared, which have trisaccharide repeating units that contained →3)-β-D-Qui*p*NAc4NAc-(1→3)-β-D-Gal*p*NAc-(1→ corresponding to the **B**→**A** structural element of *C. psychrerythraea* 34H (Schäffer et al. 2001). The chemical shifts

of C2 – C4 of residue **A** each differed by ≤ 0.5 compared those of the linear polysaccharide from *B. licheniformis* ATCC 9945 supporting that residue **B** has the D absolute configuration. In addition, another structurally modified polysaccharide from *Idiomarina abyssalis* KMM 227^T also having a linear trisaccharide repeating unit (Kokoulin et al. 2015) but this time with the β-D-Glc*p*NAcA-(1→3)-β-D-Qui*p*NAc4NAc-(1→ structural element corresponding to **C→B** in *C. psychrerythraea* 34H. The ^{13}C chemical shift differences between the two polymers were C1 in residue **C** and C2 – C4 in residue **B** differing by ≤ 0.6 ppm, thereby confirming the absolute configuration as D for the bacillosamine residue.
The substitution of all the residues by *N*-acetyl groups was confirmed by a ^{1}H,^{1}H-NOESY experiment, acquired in a H_2O:D_2O solvent mixture (Fig. 4), and a ^{1}H,^{13}C-BSCT-HMBC (Band Selective Constant Time-HMBC) experiment. In particular, correlations attributed to NH, CH_3 and COOH groups were found. Cross-peak correlations corresponding to NH/CH_3 at 8.47/2.04 ppm, 8.28/1.98 ppm, and 8.09/2.08 ppm were attributed to C*H*$_3$CO(*N*-2) of residue **B**, C*H*$_3$CO(*N*-2) of residue **C**, and C*H*$_3$CO(*N*-2) of residue **A**, respectively. By comparison, the signal at δ 8.11/1.97 ppm showed a correlation with H-6 of **B**, and is therefore attributed to C*H*$_3$CO(*N*-4) of residue **B**.
Thus, the structure of the CPS from *C. psychrerythraea* is given by →4)-β-D-Glc*p*NAcA-(1→3)-β-D-Qui*p*NAc4NAc-(1→3)-β-D-Gal*p*NAc-(1→, with the sequence of residues being ---**C**–**B**–**A**--- from the terminal end towards the reducing end of the polysaccharide (Fig. 5).

3D model of CPS

A 3D model of the polysaccharide was generated by the computer program CarbBuilder with a single command line input, (Kuttel et al. 2016) which, in its more recent form, efficiently can handle potential steric clashes between sugar residues. The 3D structure made by the program consisted of ten repeating units with dihedral angles ϕ = 40.1° and ψ = 10.0° at all glycosidic linkage using the definition commonly employed in NMR studies of oligo- and polysaccharides, namely, H1'-C1'-O*n*-C*n* and C1'-O*n*-C*n*-H*n*, where *n* denotes the substitution position, respectively (Fig. 6). These dihedral angles correspond to the *exo*-anomeric conformation for ϕ and together the synperiplanar conformation for ψ the anomeric proton and the proton on the glycosyloxylated carbon atom are in close spatial proximity, also referred to as a *syn*-conformation (Dixon et al.2003; Yang et al. 2016).
As a basis for evaluation of this model ^{1}H,^{1}H-NOESY data were analyzed using both D_2O as well as H_2O as solvents. In the former case conspicuous NOEs were observed from the anomeric protons to the protons at the linkage positions of the subsequent sugar residue (Table 1), consistent with the presence of *syn*-conformations. Interestingly, the geometrical arrangement in the 3D model of the CPS predicts that additional NOE correlations would be possible to detect from residue **B**, namely, for its methyl group at position 6 (denoted B6) to H-4 of residue **A** (cf. Fig. 4a, upper right corner) as an inter-residual NOE, from the methyl group of the *N*-acetyl group at position 2 (denoted BMe_2) to the anomeric proton H-1 of residue **C** (cf. Fig. 4a, lower left corner) and to the amino proton of the *N*-acetyl group (denoted CNH) of residue **C** (cf. Fig. 4b, middle of panel); the basis of these NOE correlations are highlighted in Figure 5 and are fully consistent with the proposed 3D model of the CPS, which when built of ten repeating units a helical structure emerges (Fig. 6). The combination of molecular mechanics-based models and NOE data can thus generate insights on both local as well as long-range structure (Sarkar et al. 2013).

Ice recrystallization inhibition assay

To evaluate if this polysaccharide had a role in cryoprotection, or the capability to interact with ice, it was tested for ice recrystallization inhibition (IRI) activity (Congdon et al. 2013). IRI is a property typically associated with antifreeze (glyco)proteins (AF(G)P) but it has been shown that several synthetic materials can also display this activity suggesting that it is more common than previously thought. IRI has also been shown to be useful in cryopreservation by reducing ice growth, in particular, upon thawing. In particular, it has emerged that synthetic materials with significantly less IRI activity than natural AF(G)Ps can also be effective cryopreservatives. To evaluate the activity of the polysaccharide investigated here, a modified splat assay was used. In short, a small droplet in PBS was used to make a polynucleated ice

wafer. This was then annealed for 30 min at -8 °C after which the amount of ice crystals formed were measured; inhibition is reported relative to PBS. As shown in Fig.7, there was relatively low activity, with a mean largest grain size above 70 % relative to PBS at 10 mg·mL^{-1}. This activity was rapidly falling off as the concentration was decreased.

Conclusions

In this study, the structural characterization of a capsular polysaccharide produced by *Colwellia psychrerythraea* 34H, grown at 8°C, is reported. The CPS shows a trisaccharide repeating unit containing galactosamine, bacillosamine and glucosaminuronic acid residues, and the 3D model suggests a helical structure. Ice recrystallization inhibition assay indicated almost no antifreeze activity for this polymer. This was unexpected, as another polymer endowed with a helical structure, i.e. the EPS isolated from *Colwellia* grown at 4°C, showed a considerable antifreeze activity. It is noteworthy that the primary structure of the molecule described in the present ~~paper~~ study does not share with the already characterized CPS and EPS the single amino acid decoration~~s~~. Thus, it is possible that the presence of alanine and threonine motifs may confer the optimum structural balance between the hydrophobic and hydrophilic regions necessary to the inhibition of ice crystals development.

Acknowledgements

This work was supported by grants from the Swedish Research Council and the Knut and Alice Wallenberg Foundation.

References

Bakermans C, Nealson KH (2004) Relationship of critical temperature to macromolecular synthesis and growth yield in *Psychrobacter cryopegella* J Bacteriol 186: 2340-2345

Bock K, Pedersen C (1983) Carbon-13 nuclear resonance spectroscopy of monosaccharides Adv Carbohyd Chem Bi 41: 27-66

Bowman JP (2014) The family *Colwelliaceae*. In Rosenberg E (ed) The prokaryotes: *Gammaproteobacteria* Springer, Berlin, Heidelberg pp 179-193

Carillo S, Casillo A, Pieretti G, et al. (2015). A unique capsular polysaccharide structure from the psychrophilic marine bacterium *Colwellia psychrerythraea* 34H that mimics antifreeze (Glyco)proteins J Am Chem Soc 137: 179-189

Carillo S, Pieretti G, Lindner B, et al. (2013). Structural characterization of the core oligosaccharide isolated from the lipopolysaccharide of the psychrophilic bacterium *Colwellia psychrerythraea* strain 34H. Eur J Org Chem 18: 3771-3779

Casillo A, Parrilli E, Sannino F, et al. (2017) Structure-activity relationship of the exopolysaccharide from a psychrophilic bacterium: a strategy for cryoprotection Carbohydr Polym 156: 364-371

Cavicchioli R, Thomas T (2000) Extremophiles. In: Lederberg J, Alexander M, Bloom BR, Hopwood D, Hull R, Iglewski BH, Laskin AI, Oliver SG, Schaechter M, Summers WC. (ed) Encylopedia of Microbiology, 2rd edn. Academic Press Inc, San Diego, pp 317-337.

Congdon TC, Notman R, Gibson MI (2013). Antifreeze (Glyco)protein mimetic behavior of poly(vinyl alcohol): detailed structure ice recrystallization inhibition activity study Biomacromolecules 14(5): 1578-1586

Corsaro MM, Grant WD, Grant S, Marciano CE, Parrilli M (1999) Structure determination of an exopolysaccharide from an alkaliphilic bacterium closely related to *Bacillus* spp Eur J Biochem 264: 554-561

D'Alonzo D, Cipolletti M, Tarantino G, et al. (2016) A semisynthetic approach to new immunoadjuvant candidates: site-selective chemical manipulation of *Escherichia coli* monophosphoryl lipid A Chem Eur J 22:1-12

De Mayeer P, Anderson D, Cary C, Cowan DA (2014) Some like it cold: understanding the survival strategies of psychrophiles EMBO reports 15: 508-517

de Pinto MC, Lavermicocca P, Evidente A, Corsaro MM, Lazzaroni S, De Gara L (2003) Exopolysaccharides Produced by Plant Pathogenic Bacteria Affect Ascorbate Metabolism in *Nicotiana tabacum* Plant Cell Physiol 44: 803-810

Decho AW (1990) Microbial exopolymer secretions in ocean environments: their role(s) in food webs and marine processes. In Barnes M (ed) Oceanography and Marine Biology: an Annual Review. Aberdeen Univ Press, UK, pp. 73-153.

Deming JW, Somers LK,. Straube WL, et al. (1988) Isolation of an obligately barophilc bacterium and description of a new genus *Colwellia* gen. nov. Syst Appl Microbiol 10:152-160

Dixon AM, Venable R, Widmalm G, Bull TE, Pastor RW (2003) Application of NMR, Molecular simulation, and hydrodynamics to conformational analysis of trisaccharides Biopolymers 69(4): 448–460

Ewert M, Deming JW (2013) Sea ice microorganisms: Environmental constraints and extracellular responses Biology 2: 603-628

Findeisen M, Brand T, Berger S (2007) A ^{1}H-NMR thermometer suitable for cryoprobes Magn Reson Chem 45: 175-178

Fux CA, Stoodley P, Hall-Stoodley L (2003) Bacterial biofilms: a diagnostic and therapeutic challenge Expert Rev Anti Infect Ther 1: 667-683

Galanos C, Lüderitz O, Westphal O (1969) A New Method for the Extraction of R Lipopolysaccharides Eur J Biochem 9: 245-249

Huston AL, Methè BA, Deming JW (2004). Purification, characterization, and sequencing of an extracellular cold-active aminopeptidase produced by marine psychrophile *Colwellia psychrerythraea* strain 34H Appl Environ Microb 70: 3321-3328

Jansson P, Kenne L, Widmalm G (1989) Computer-assisted structural analysis of polysaccharides with an extended version of CASPER using ^{1}H- and ^{13}C NM.R data Carbohyd Res 188: 169-191

Jansson P, Kenne L, Widmalm G (1991) CASPER: A computer program used for structural analysis of carbohydrates J Chem Inf Comput Sci 31: 508-5 16

Kadioglu A, Weiser JN, Paton JC, Andrew PW (2008) The role of Streptococcus pneumoniae virulence factors in host respiratory colonization and disease Nat Rev Microbiol 6: 288-301

Kokoulin MS, Komandrova NA , Kalinovskiy AI, Tomshich SV , Romanenko LA, Vaskovsky VV (2015) Structure of the O-specific polysaccharide from the deep-sea marine bacterium Idiomarina abyssalis KMM 227T containing a 2-O-sulfate-3-N-(4-hydroxybutanoyl)-3,6-dideoxy-D-glucose Carbohyd Res 413: 100-106

Kumar AS, Mody K, Jha B **(**2007) Bacterial exopolysaccharides – a perception J Basic Microb 47: 103-117

Kuttel MM, Ståhle J, Widmalm G (2016) CarbBuilder: Software for building molecular models of complex oligo- and polysaccharide structures *J* Comput Chem 37: 2098-2105

Laemmli UK. (1970). Cleavage of structural proteins during the assembly of the head of bacteriophage T4 Nature 227 680-685

Leontein K, Lindberg B, Lönngren J (1978) Assignment of absolute configuration of sugar by g.l.c. of their acetylated glycosides from chiral alcohols Carbohydr Res 1978 62: 359-362

Lipkind GM, Shashkov AS, Knirel YA, Vinogradov E, Kochetkov NK (1988) A computer-assisted structural analysis of regular polysaccharides on the basis of ^{13}C-NMR data. Carbohyd Res 175: 59-75

Liu SB., Chen XL, He HL et al. (2013). Structure and ecological roles of a novel exopolysaccharide from the Arctic sea ice bacterium *Pseudoalteromonas* sp. Strain SM20310 Appl Environ Microb 79(1): 224-230

Lundborg M, Widmalm G (2011) Structural analysis of glycans by NMR chemical shift prediction Anal Chem 83: 1514-1517

Mancuso Nichols CA, Guezennec J, Bowman JP (2005) Bacterial exopolysaccharides from extreme marine environments with special consideration of the southern ocean, sea ice, and deep-sea hydrothermal vents: A review Mar Biotechnol 7: 253-271

~~Marx JD, Carpenter SD, Deming JW (2009). Production of cryoprotectant extracellular polysaccharide substances (EPS) by the marine psychrophilic bacterium *Colwellia psychrerythraea* strain 34H under extreme conditions. Can J Microbiol 55: 63-72~~

Methé BA, Nelson KE, Deming JW, et al. (2005) The psychrophilic lifestyle as revealed by the genome sequence of *Colwellia psychrerythraea* 34H through genomic and proteomic analyses. Proc Natl Acad Sci U.S.A. 102: 10913-10918

Pieretti G, Corsaro MM, Lanzetta R, et al. (2009) Structure of the core region from the lipopolysaccharide of *Plesiomonas shigelloides* Strain 302-73 (Serotype O1) Eur J Org Chem 1365-1371

~~Pieretti G, Corsaro MM, Lanzetta R, Parrilli M, Canals R, Merino S, Tomás JM (2008) Structural studies of the O-chain polysaccharide from *Plesiomonas shigelloides* Strain 302-73 (Serotype O1) Eur J Org Chem 3149-3155~~

Poli A, Anzelmo G, Nicolaus B (2010) Bacterial exopolysaccharides from extreme marine habitats: production, characterization and biological activities Marine drugs 8: 1779-1802

Sarkar A, Fontana C, Imberty A, Pérez S, Widmalm G (2013) Conformational preferences of the O-antigen polysaccharides of *Escherichia co*li O5ac and O5ab using NMR spectroscopy and molecular modeling Biomacromolecules 14: 2215−2224

Schäffer C, Scherf T, Christian R, Kosma P, Zayni S, Messner P, Sharon N (2001) Purification and structure elucidation of the N-acetylbacillosamine-containing polysaccharide from Bacillus licheniformis ATCC 9945 Eur J Biochem 268: 857-864

Söderman P, Jansson P, Widmalm G (1998) Synthesis, NMR spectroscopy and conformational studies of the four anomeric methyl glycosides of the trisaccharide D-Glc*p*-(1→3)-[D-Glc*p*-(1→4)]-α-D-Glc*p* J Chem Soc Perkin Trans 2

Sutherland IW (1982) Biosynthesis of microbial exopolysaccharides Adv Microb Phys 23: 79-150

Westphal O (1965) Bacterial lipopolysaccharide-extraction with phenol water and further application of procedure Methods Carbohydr Chem 5: 83-91

Widmalm G (2007) General NMR spectroscopy of carbohydrates and conformational analysis in solution. In Comprehensive glycoscience, J. P. Kamerling, Ed., Elsevier, Oxford, Vol. 2,pp. 101-132.

Yang M, Angles d'Ortoli T, Säwén E, Jana M, Widmalm G, MacKerell Jr AD (2016) Delineating the conformational flexibility of trisaccharides from NMR spectroscopy experiments and computer simulations Phys Chem Chem Phys 18: 18776-18794

Figure legends

Fig. 1 DOC-PAGE analysis of the CPS fraction from *C. psychrerythraea* 34H grown at 8 °C (a) and 4 °C (b). The gel was stained with Alcian blue dye.

Fig. 2 Diffusion-filtered ^{1}H NMR spectrum recorded at 310 K of the CPS from *C. psychrerythraea* 34H grown at 8 °C. The anomeric signals from the three sugar residues are annotated **A** – **C**.

Fig. 3 Multiplicity-edited ^{1}H,^{13}C-HSQC NMR spectrum of the CPS from *C. psychrerythraea* 34H grown at 8 °C showing (a) the anomeric signals, ring region with methylene groups in red, nitrogen-bearing carbons and (b) methyl groups; in (c) correlations are shown of a ^{1}H,^{13}C-band-selective constant-time HMBC NMR experiment for methyl-carbonyl connectivities of the *N*-acetyl groups.

Fig. 4 Selected regions of a ^{1}H,^{1}H-NOESY NMR spectrum of the CPS from *C. psychrerythraea* 34H grown at 8 °C recorded at 5 °C in a 95:5 H_2O:D_2O mixture, using a mixing time of 300 ms, showing (a) the inter-residual (colored purple) correlations from bacillosamine CH_3 groups. In (b) and (c) correlations from *N*-acetyl amino protons, intra-residual in black and inter-residual in purple, can be seen.

Fig. 5 Primary repeating trisaccharide structure of the CPS from *C. psychrerythraea* 34H grown at 8 °C.

Fig. 6 A 3D model of the CPS from *C. psychrerythraea* 34H grown at 8 °C generated by CarbBuilder v2.1.7 and visualized with PyMol 1.3 with a single repeating unit highlighted. Inter-residual correlations shown in purple in Figure 4 are represented by dashed lines. To the right is a ten-repeat CPS displayed in CPK form, showing a helical structure.

Fig. 7 Ice Recrystallization Inhibition activity of CPS from *C. psychrerythraea* 34H grown at 8 °C was compared with PEG, used as a negative control, and PVA as a positive. Mean largest grain size is expressed as a percentage of PBS buffer, and a small mean largest grain size (MLGS) value indicate increased IRI activity.

Figures

Fig. 1

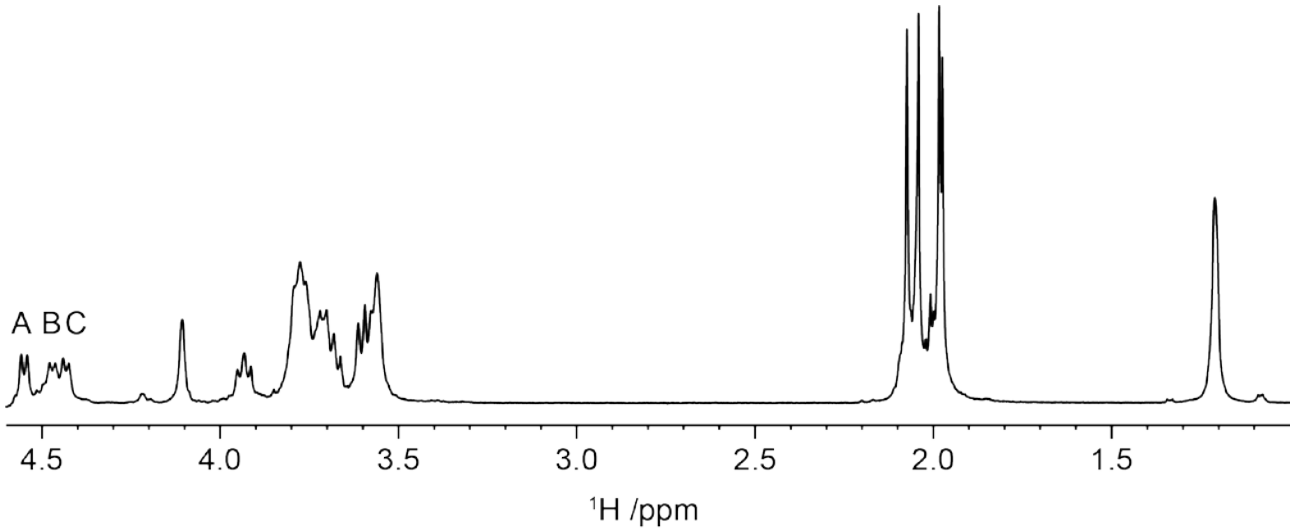

Fig. 2

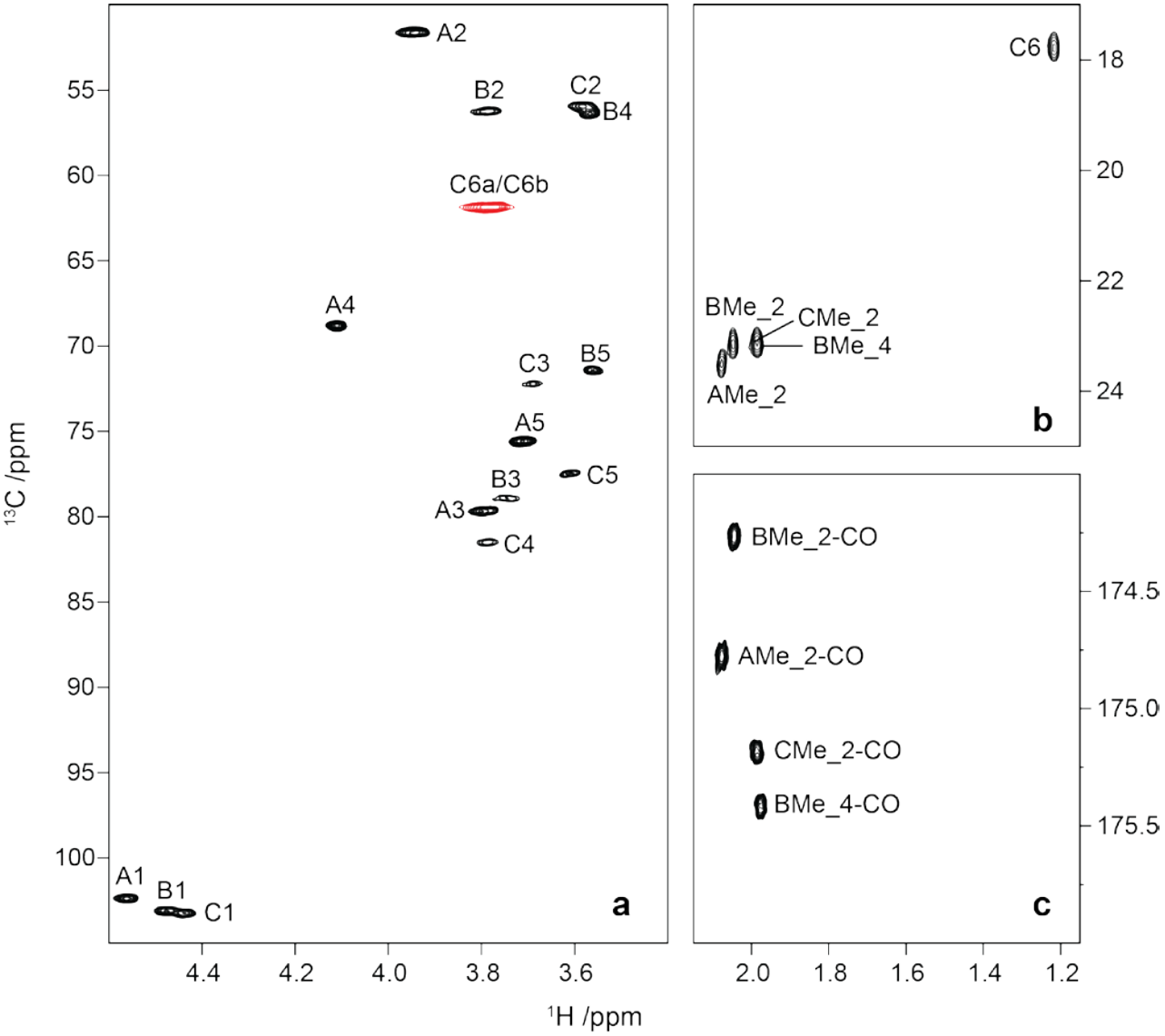
A2
B2
C2
B4
C6a/C6b
A4
C3
B5
A5
B3
C5
A3
C4
A1
B1
C1
a
^{13}C /ppm
^{1}H /ppm
C6
BMe_2
CMe_2
BMe_4
AMe_2
b
BMe_2-CO
AMe_2-CO
CMe_2-CO
BMe_4-CO
c

Fig. 3

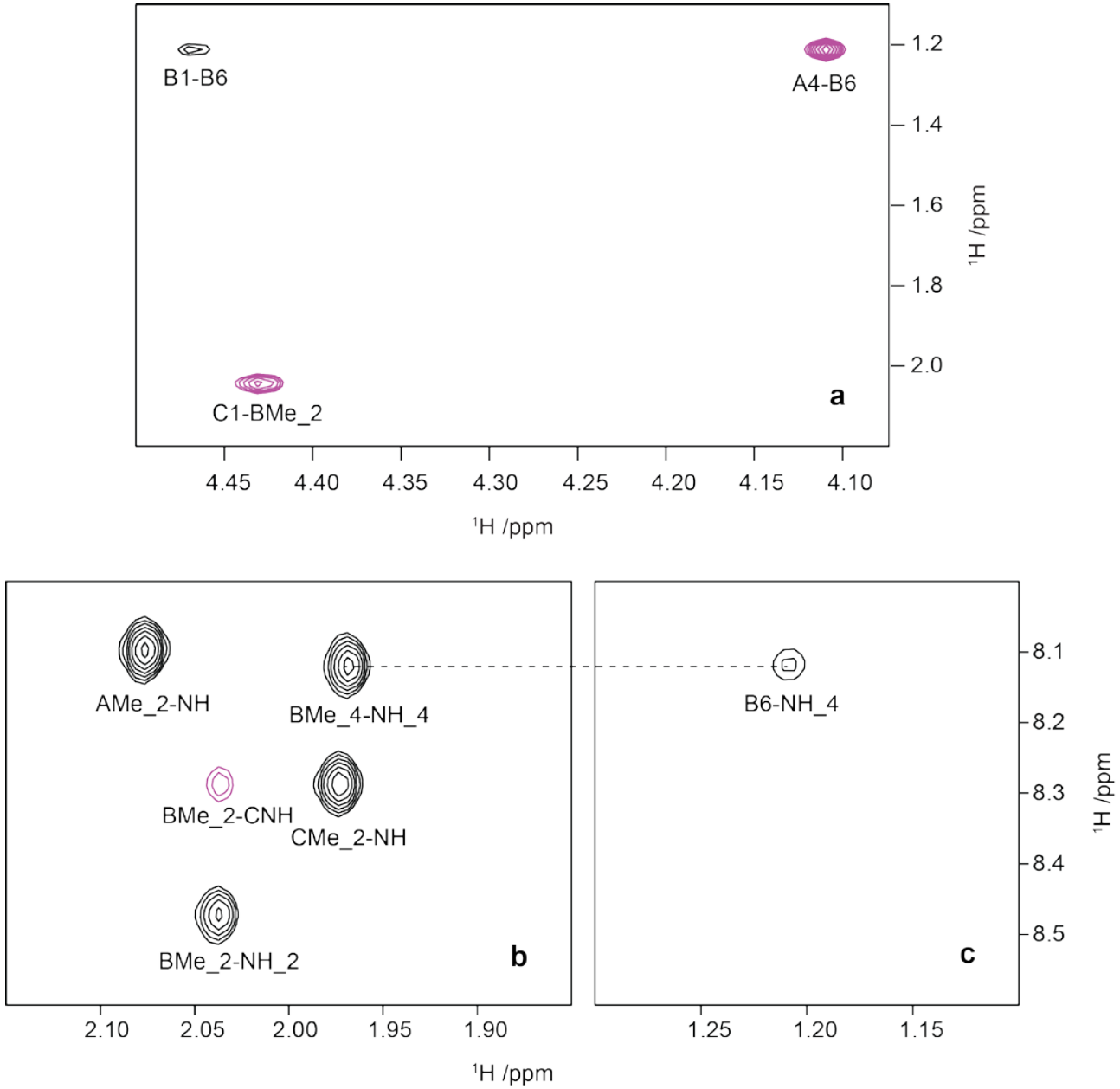
B1-B6
A4-B6
C1-BMe_2
a
1.2
1.4
1.6
1.8
2.0
¹H /ppm
4.45
4.40
4.35
4.30
4.25
4.20
4.15
4.10
¹H /ppm
AMe_2-NH
BMe_4-NH_4
BMe_2-CNH
CMe_2-NH
BMe_2-NH_2
b
B6-NH_4
c
8.1
8.2
8.3
8.4
8.5
¹H /ppm
2.10
2.05
2.00
1.95
1.90
1.25
1.20
1.15
¹H /ppm

Fig. 4

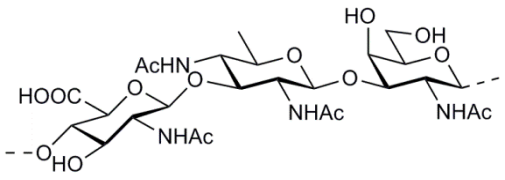
HO
OH
AcHN
O
HOOC
NHAc
NHAc
NHAc
HO

Fig. 5

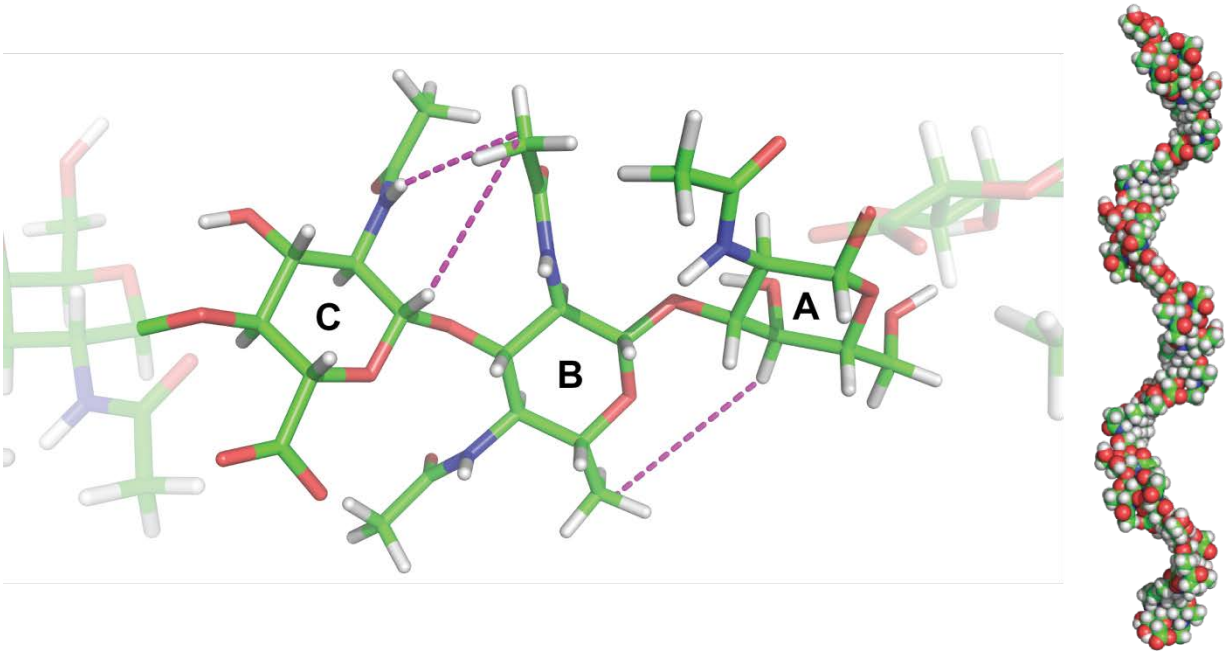
C
B
A

Fig. 6

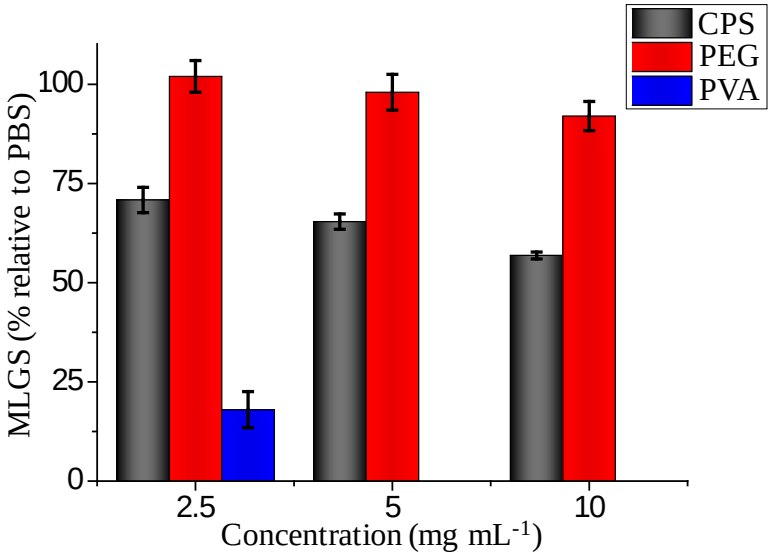
CPS
PEG
PVA
MLGS (% relative to PBS)
0
25
50
75
100
2.5
5
10
Concentration (mg mL-1)

Fig. 7

Table 1

^{1}H and ^{13}C NMR chemical shift (ppm) assignments of CPS from *C. psychrerythraea* 34H grown at 8 °C. Spectra were acquired in D_2O solution at 310 K.

Sugar residue		^{1}H/^{13}C											Correlation to atom (from anomeric atom)	
		1	2	3	4	5	6	C*H*$_3$CO *N*-2	CH$_3$*C*O *N*-2	C*H*$_3$CO *N*-4	CH$_3$*C*O *N*-4	NH[a]	NOE	HMBC
→3)-β-D-Gal*p*NAc-(1→	**A**	4.55[8.4]	3.93	3.79	4.11	3.70	3.76, 3.78	2.08				8.09(*N*-2)	H4, **C**	C4, **C**
		(–0.13)	(0.03)	(0.02)		(–0.02)		(–0.01)					H3, **A**	H4, **C**
		102.5	51.8	79.7	68.8	75.6	61.9	23.6	175.1					
		(6.2)	(–3.0)	(7.7)	(–0.1)	(–0.4)	(0.0)	(0.5)	(–0.7)					
→3)-β-D-QuiNAc4NAc-(1→	**B**	4.47[8.0]	3.78	3.73	3.56	3.55	1.21	2.04		1.97		8.47(*N*-2)	H3, **A**	
		103.1	56.3	78.9	56.5	71.5	17.9	23.3	174.6	23.3	175.9	8.11(*N*-4)		
→4)-β-D-Glc*p*NAcA-(1→	**C**	4.43[7.3]	3.58	3.68	3.77	3.60		1.98				8.28(*N*-2)	H3, **B**	C3, **B**
		(–0.30)	(–0.12)	(0.10)	(0.19)	(–0.12)							H3, **C**	
		103.3	56.0	72.3	81.6	77.6	174.3	23.3	175.5					
		(7.5)	(–1.7)	(–2.3)	(8.0)	(0.6)	(–1.2)	(0.2)	(–1.9)					

[3] $^{3}J_{H1,H2}$ values are given in Hertz in square brackets. Chemical shift differences as compared to corresponding monosaccharides and are given in parentheses.(Jansson et al. 1989, Lundborg et al. 2011)

[a] Assignments based on a ^{1}H,^{1}H-NOESY experiment at 5 °C with τ_m = 300 ms using a H_2O:D_2O solvent mixture of 95:5.